T. Jones (5)

MINNEAPOLIS HONEYWELL REGULATOR COMPANY
AERO ENGINEERING DOCUMENT R-ED- 9230

DOCUMENT NUMBER: R-ED-9230

TITLE: MH 64
G LIMITER STATUS REPORT

DATE: 6 December 1957

Prepared by Donald Eckert
Donald Eckert
Sr. Systems Analyst

Prepared by Marlowe W. Iverson
Marlowe W. Iverson
Sr. Systems Engineer

Approved by R G Patterson
R. G. Patterson
Systems Project Engineer

Approved by L. Prince
L. Prince
Asst. Project Engineer Analysis

TL 113-57/12

~~RL. 47~~

ABSTRACT

This document is a status report on the pitch acceleration limiter for the MH-64 and covers the following subjects:

1.0 REAC STUDY

2.0 ERROR ANALYSIS - A COMPILATION OF DEVICE TEST DATA AND A CALCULATION OF THE RESULTANT SYSTEM ERROR

3.0 EFFECTS OF SYSTEM ERRORS ON SYSTEM PERFORMANCE

4.0 GROSS WEIGHT AND C.G. CONSIDERATIONS

5.0 STATEMENT OF OUTSTANDING PROBLEMS

6.0 RECOMMENDED APPROACHES TO THE SOLUTION OF THE OUTSTANDING PROBLEMS

Section 1.0, REAC STUDY, contains exerpts from the G-Limiter Analytical Report which although yet published, is in the process of preparation.

1.0 REAC STUDY

A brief resume' of computer results and work in process is included as part of the status report in order to delineate some of the existing problems.

The limit function containing the $\frac{162}{32.2}\dot{q}$ term has been on the REAC four times.

1. Main Analysis (See REAC Diagram figure 1)

   Considered .100 seconds delay on both servos. δ_D centering in .250 seconds and δ_p at 40°/sec.

2. 1st Revision

   Revised δ_D centering to .600 seconds.

3. 2nd Revision

   Used .020 second delay due to relays; .030 second delay on parallel servo disengagement. Used .016 second lag for mag amp.

4. 3rd Revision (See REAC Diagram Figures 2 & 3)

   Is using .020 second delay due to relays; .030 second delay on each servo, .300 and .600 second return rate on δ_D and 40°/sec return rate on δ_p. Also adds accelerometer and rate gyro dynamics, rate limiting on servos and H.M. effects on surface. Uses .033 second lag on pre-amp - mag-amp combination.

1.1 Curves of N_z vs δ_e.

1.1.1 Main Analysis and 1st Revision

Results of the main analysis and 1st revision are given in figures 4 - 9 for a .31$\bar{c}$ and 47,000 lb. G.W.

Results of a .27 and .35$\bar{c}$ are given in figures 10,11 and 12 for a limited number of conditions.

1.1.2 2nd Revision

The results of the second revision are given by the solid dot curves of figures 13 and 14 It is to be noted that this mechanization did not allow for a .030 second differential servo dead time.

3 3rd Revision

The REAC work on the third revision is still in process. The results can be made available at the end of December if it is decided at the 9 December analytical meeting to continue this study. .

1.2 Discussion of Results

It is to be noted that these curves of computer results are based on an ideal system with no errors. Refer to section 2.0 for a statement of system error and section 3.0 for the effects that system error have on system performance.

2.0 ERROR ANALYSIS

The present limit function for the pitch acceleration limiter for the MH64 Damper is as follows:

$$L = \left(\triangle Nz + \frac{162\dot{q}}{32.2}\right)\frac{1 + 0.02s}{1 + 0.1s} + 12.5\,\delta_D\,\frac{2s}{1 + 2s} + 15.75\,\delta_p\,\frac{.5s}{1 + 5s}$$

The following error analysis is predicated on the use of GG47E Accelerometer, on LG16 position transmitter and a BG47E calibrator in a duplicate failsafe system.

2.1 Individual Errors

2.1.1 Accelerometer linearity

The manner in which the limit function is derived may be shown as follows:

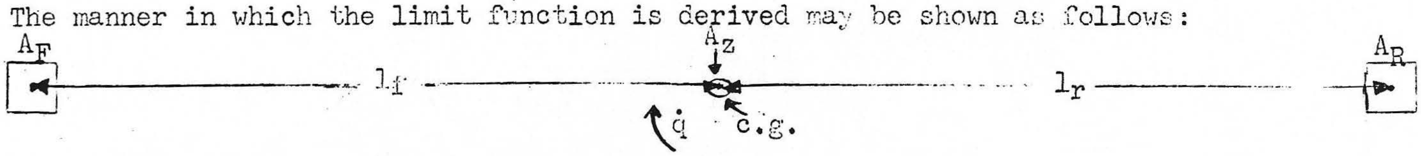

(a) $A_F = A_z + l_f\,\dot{q}$

(b) $A_R = A_z - l_r\,\dot{q}$

(c) $K_R A_R = K_R\,(A_z - l_r\,\dot{q})$ wherein K_R is the attenuation factor of A_R relative to A_F as determined in the bridge.

(d) Subtracting (c) from (a)

$$AF - K_R A_R = A_z\,(1 - K_R) + (l_f + K_R l_r)\,\dot{q}$$

(e) Dividing by $1 - K_R$

$$\frac{A_F - K_R A_R}{1 - K_R} = A_2 + \frac{l_f + K_R l_r}{1 - K_R}\,\dot{q}$$

(f) Allowing for the bridge mechanization and the addition of high passed servo terms equation (e) becomes:

$$\frac{e_m}{K_b} = \frac{A_F - K_R A_R}{1 - K_R} = \left[A_z + \frac{l_f + K_R l_r}{1 - K_R}\,\dot{q}\right]\frac{1 + T_1 s}{1 + NT_1 s} + \delta_D\,\frac{T_2 s}{1 + T_2 s} + \delta_p\,\frac{T_3 s}{1 + T_3 s}$$

wherein e_n is the bridge voltage and K_b the proportionality factor.

(g) In the CF-105 installation the accelerometers are located 22 feet forward and 7 feet aft of the 31% c.g.

The previously proposed limit function has a $\dot{q}$ gain of 162 or solving for K_R ;-

(1) $$\frac{l_f + K_R l_r}{1 - K_R} = 162 = \frac{22 + 7K_R}{1 - K_R}$$

2.1.1 (cont.)

(g) (cont.)

(2) $162 - 162K_R = 22 + 7K_R$

$$K_R = \frac{140}{169} = 0.828$$

(h) If we assume $\mathring{i} = \mathring{\delta}_D = \mathring{\S}_p = 0$, and $A_z = A_L$ wherein A_L is the limit A_z;

$$\frac{A_F - K_R A_R}{1 - K_R} = A_z = A_L$$

For a ±.1g error in absolute accelerometer linearity ;

$$\frac{\triangle A_F - K_R \triangle A_R}{1 - K_R} = \triangle A_{L_1}$$

$$\frac{\pm .1\ (1 + .828)}{1 - .828} = \triangle A_{L_1}$$

$$\triangle A_{L_1} = \pm \frac{.1 \times 1.828}{.172} = \pm 1.06 \text{ g's}$$

$$E_a = \pm 1.06 \text{ g's}$$

(i) The ±.1g absolute linearity has components as follows:

(1) ± .05 g resolution max

(2) ± .08 g linearity at room temperature

(3) ± .07 g temperature effects

At present the accelerometer manufacturer has to compensate each device by selection of end resistors to get the combination of effects to yield a ±.1g absolute linearity unit. Thus even with the addition of heaters and use of matched accelerometers it is doubtful that an absolute linearity of smaller than ±.08 g's could be achieved especially in view of the ±0.05 g threshold.

The error for a ±.08g accelerometer would be:

$$\triangle A_{L_1} = \frac{\pm .08 \times 1.828}{.172} = \pm .85 \text{ g's}$$

E_a = ±.85 g's with matched accelerometer

2.1.1 (cont.)

(i) (cont.)

It is to be noted that ΔA_{L_1} is a maximum error occuring for $\omega = o$ since $s = j\omega$

$$A_L = \frac{A_F - K_R A_R}{1 - K_R} \cdot \frac{1 + .02s}{1 + .1s}$$

At $\omega = \infty$ $\quad A_L = A_{L_1} \times \frac{1}{5}$

In the case of failures $\omega = f(\dot{\delta}_s)$ and in actuality increases with $\dot{\delta}_s$. Another factor which makes matching impractical is due to the duplicate nature of the system. Each accelerometer has two potentiometer pick-offs, necessitating the matching of two sets of pick-offs between the two accelerometers. Thus if there is N probability of securing a match in a given lot of accelerometers to a level of accuracy A between two potentiometers, one on each accelerometer, the probability of securing a match between two sets is N^2 where N is a number less than unity.

2.2 Temperature Sensitive Errors

	-65°F	75°F	160°F	Notes
Mag Amp	+0.14	0	+0.14	See figure 15 & 16
Pre-Amp	-0.05	0	0	See figure 17
Accelerometer Damping	+ .1g	0	-.2g	*
Total Effect	+ .19g	0	-.06g	

*Accelerometer damping ratio data was obtained from a previous system which used identical accelerometers and a similar limit function. Accelerometer temperature effects on linearity have been included under absolute linearity errors due to the random nature of the effect.

$E_{T_{max}} = 0.19g$'s $\qquad E_{T_{mo}} \Big|_{140°F} = -.03g$'s

2.3 Errors due to a.c. line voltage variations

	102v	115v	121v	Notes
Pre Amp	-.05g's	0	+.05g's	See figure 15
Mag Amp	+.08g's	0	-.08g's	See figures 16 & 17
	+.03g's	0	+.03g's	

E_v =.03g's

2.4 Calibration Error

Based on experience with previous systems the closest that a system can be calibrated for field use is ±0.1g's.

$E_c = \pm$ 0.1g's

2.5 Other Errors

A number of other sources of error exist which have not been fully evaluated and are listed as follows:

(a) Disengage Time Errors

(b) Tolerance on δ_e due to tolerances in aircraft control system.

*(c) Bridge Variations (R-C tolerances)

(d) Apparent error on $\dot{q}$ due to differences in temperature environments of fore and aft accelerometers $\delta = f(T)$

*(e) Line frequency variations

*(f) Aging effects

*These errors are small enough so as not to have an appreciable effect on overall system error.

2.6 Error Summary

2.6.1 The "least squares" method of error analysis may be used when the following conditions exist.

(a) Normal error distribution of each variable

(b) No significant correlation between variables

Thus if $A = X + Y$

$\Delta A = \sqrt{(\Delta X)^2 + (\Delta Y)^2}$ providing the conditions of (a) and (b), above are met.

2.6.2 When an error has a skewed distribution on a frequency occurance basis it may be treated as follows:

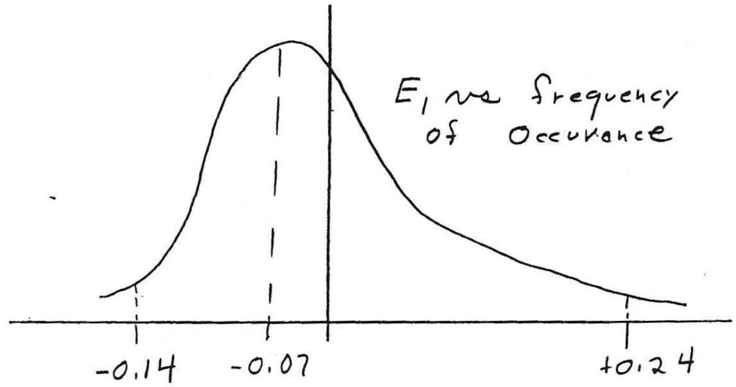

$E_T = E_1 + E_2$ wherein E_2 has a normal distribution

$$E_T = E_{1_{mo}} \pm \sqrt{E_1\ max^2 + E_2^2}$$

$$E_T = -0.7 \pm \sqrt{0.24^2 + E_2^2}$$

2.6.3 Tabulation of Errors

Symbol	Source	Max Value	Modal Value	Distribution
E_a	Accelerometer Linearity with	±1.06g	0	normal
	matched accelerometers	±0.85g	0	normal
E_T	Temperature variation	+0.19g	-.03g	skewed
E_V	Voltage variations	+.03	0	inverted
E_c	Calibration	± 0.1	0	normal

With unmatched accelerometers total system error is:

$$E_{Total} = -.03 \pm \sqrt{(1.06)^2 + (.19)^2 + (0.03)^2 + (0.1)^2}$$

$$E_{Total} = \begin{matrix} +1.05 \\ -1.11\text{g's} \end{matrix}\ \text{max}$$

With matched accelerometers total system error is:

$$E_{Total} = -.03 \pm \sqrt{(0.85)^2 + (0.19)^2 + (0.03)^2 + (0.1)^2}$$

$$E_{Total} = \begin{matrix} +.85 \\ -.91\ \text{g's max} \end{matrix}$$

3.0 EFFECTS OF SYSTEM ERRORS ON SYSTEM PERFORMANCE

Figure 18 is a partial replot of figure 13 to show the approximate effect of errors as derived in section 2.0 on system performance. It will be noted that the errors used are those that would be associated with a system utilizing matched accelerometers.

Referring to figure 18, curve 1 is the theoretical peak g curve for a 35% c.g. 47,000 lb. GW. Curve 2 is the theoretical peak g curve for a 27% c.g., 47,000 lb. gross weight. The G Limiter Calibrator must be set at 6.0 - 0.85 g's or 5.15 g's in order that curve (1) not be raised to a higher g level. This is shown by curve 3 as the nominal peak g's; curves 2 and 4 requesting the tolerance band about curve 3.

In actually curves 3 and 4 will converge slightly toward curve 2 as a function of increasing $\dot{\delta}_e$ inasmuch as there is a lag network on $A_z + K\dot{q}$, but this would not be likely to be appreciable.

Thus it may be seen that if the present G Limiter is set to assure that peak g's do not exceed curve 1 for condition 20.9 - .35$\bar{c}$,that disengagements could occur as low as 4 to 4.5 g's absolute for .27$\bar{c}$. This does not even consider the problems of gusts or structural pick up.

An examination of the N_z vs $\dot{\delta}_e$ curves in section 1.0 will show that there are a number of other flight conditions where low g disengages could take place as a result of system error.

4.0 GROSS WEIGHT AND C.G. CONSIDERATIONS

During the REAC study of the limiter MH used a 47,000 lb. gross weight and a 31% c.g. A few runs were made at a 35% c.g., however.

The limit load factors MH used were those specified by AVROCAN Specification E-276 which are +7.3g's and -3.4 g's.

4.0 (Cont.)

AVRO Document P/Control 105 dated July 1957 (MH Index 105-343) shows a variable limit load factor as a function of Mach Number and Gross Weight. The gross weights given are 47,000 lbs. and 52,500 lbs. The flight envelopes reflect a minimum limit load factor of 6.8 g's and 6.0 g's respectively for these gross weights.

Recently MH has learned that the take off gross weight can be as high as 69,000 lbs. and that the landing gross weight can be as high as 60,000 lbs. The 69,000 lb. gross weight has a limit load factor of 4.6 g's.

Obviously, with our present G limiter mechanization, if we were to mechanize not to exceed 4.6 g's for the high gross weights the aircraft performance would be seriously compromised at normal gross weights.

Each c.g. position must be tied down in terms of the particular range of gross weights and flight conditions that it is associated with in order to determine an optimum g limiter mechanization.

5.0 STATEMENT OF OUTSTANDING PROBLEMS

The following is a list of the outstanding problems on the pitch acceleration limiter for the MH-64 System. The problems listed are not necessarily listed in their order of importance.

5.1 A Three Servo Ramp Input can result from a single failure in the MH64 Bridge.

The following single bridge failures will result in a three servo ramp input:

(1) Short pitch rate or normal acceleration to 115 volts anywhere between sensor pickoffs and the AG26 or pitch integrator.

(2) EG153A-2 failure with saturated output.

(3) Pitch Rate high pass runs hardover.

(4) Open circuit between pitch rate high pass and the EG153A-1.

REAC Analysis has shown that with the present $\dot{\delta}_{e_{max}}$ thereis no limit function which can protect against this failure at all flight conditions. This was substantiated by setting up the computer for a disengagement, at the instant the failure occurred the result being peak g's in excess of the limit load factor.

5.2 Increased dead time of differential servo upon disengage due to stroke change.

The stroke of the differential servo was changed from ±0.6" to ±0.375" nominal stroke. Among other effects this increased the dead time upon disengage of the differential servo. This resulted because the centering mechanism now moves through the 0.6" to 0.375" length of stroke before it starts to center the servo. The dead time increased from approximately .030 to .100 seconds or thereabouts.

5.3 The divergence of the N_2 vs $\dot{\delta}_s$ curves.

In order to completely specify the requirements for a disengage type of an anticipatory pitch acceleration limiter the g level below which nuisance disengagements cannot be tolerated must be specified in addition to the limit load factor which is not to be exceeded. This should be specified for both positive and negative loads.

The resultant g band must allow for the following:

(a) Static and dynamic system error

(b) Aerodynamic variations

(c) Gust inputs

(d) Gross weight changes

(e) C.G. shift

(f) Accelerometer output due to structural pick-up

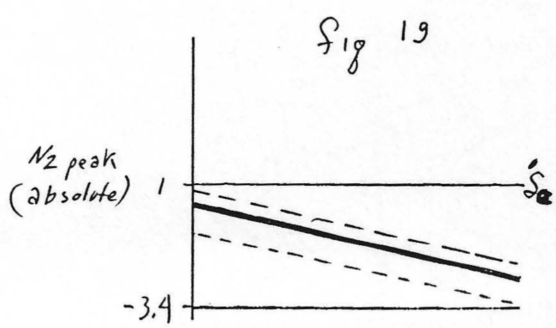

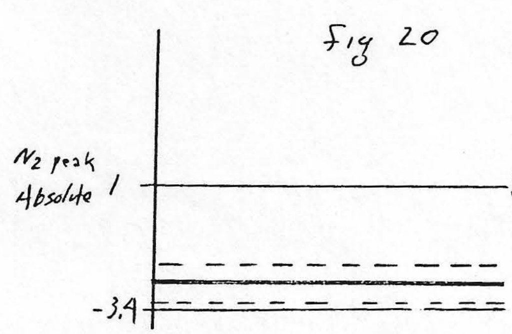

5.3 (cont.)

Figure 19, although somewhat exaggerated to clearly show the principle involved, shows that with a divergent curve it is necessary to set thelimit close to level flight conditions in order to protect for large elevator failure rates. Assuming that a curve similar to figure 20 could be developed, it can be seen that the apparent advantages would be a lesser possibility of nuisance disengagements. One of the factors which would tend to make possible the characteristics of figure 20 would be the reduction of $\dot{\delta}_{e_{max}}$.

5.4 The Effects of Maximum Elevator Rate vs Dead Time.

Regardless of the limit function mechanized, certain dead times and first order lags are going to be encountered in any type of anticipatory system. Neglecting first order lags and considering only dead times for a parallel servo failure the following dead time exists in the available hardware:

Disengage Relays	.020 seconds
Parallel Servo Disengage Delay	.030 seconds
	.050 seconds

For S.L., Mn=1.09; N_{2}/δ_e = 2g's/o, and at present $\dot{\delta}_{e_{max}}$ = 40°/sec as limited by the primary control system. The .050 second dead time therefore results in pulling 4 g's just due to dead time alone. This may be substantiated as follows:

2g's/o x 40°/sec x .050 sec = 4g's

5.5 System Error

System Error is large due primarily to the accelerometer linearity error as magnified by the necessary summing techniques to get the high $\dot{q}$ gain required to protect the aircraft with the present pitch axis mechanization (Refer to section 3.0 for further details).

5.6 Gross Weight and C.G. Variations

As stated in section 4.0 with our present mechanization setting for limits to protect the aircraft for the limit load factors associated with high gross weights, will seriously compromize the aircraft performance at low gross weights.

6.0 RECOMMENDED APPROACHES TO THE SOLUTION OF OUTSTANDING PROBLEMS

Reduction of $\dot{\delta}_e$

One important step that would make for a more acceptable g limiter, regardless of the limit function, is to reduce $\dot{\delta}_e$. Of course reducing the dead time also would be of help. But unfortunately the "state of the art" is such as to make a further reduction in dead time very unlikely.

It is proposed that AVRO and MH review the required $\dot{\delta}_{e_{max}}$ requirements in terms of desired aircraft performance to determine if a reduction in $\dot{\delta}_{e_{max}}$ is possible.

6.2 Decreased Dead Time on Differential Servo Upon Disengagements

As authorized in the November and October cocordination meetings MH is conducting a study to determine whether or not the MG51 differential servo can be changed to overcome the ill effects of the stroke change. One of the items being considered is the reduction of dead time.

System Error

Since Accelerometer Linearity is the main source of system error as magnified by the summing methods to obtain the high $\dot{q}$ gain means must be found to reduce the $\dot{q}$ gain of the limit function.

The main reason the gain was so high in the first place is that with the present pitch axis gains the aircraft is unstable for loss of pitch rate. The high gain on $\dot{q}$ in the limit function being required to provide adequate anticipation to protect against the type of failure.

MH has derived new pitch axis gains and mechanization which:

(a) Make the aircraft stable for loss of pitch rate, and

(b) Reduce the probability of a three servo hardover as the mechanization utilizes δ_{fn} but not δ_n to the differential servo as now mechanized.

The new pitch axis gains would likely allow the $\dot{q}$ gain in the limit function to be cut in half or maybe slightly more. This would allow a considerably larger reduction of system error than that which could be obtained by matching accelerometers.

.3 (cont.)

It is therefore proposed that MH conduct a study to try to determine a limit function to be used with the new pitch axis gains.

6.4 Reduction of the possibility of a three servo ramp input due to a single bridge failure.

As noted in section 6.3 if the revised pitch axis gains aremechanized a normal acceleration term is fed to the parallel servo only and not to both servos as is the case with the present pitch axis. This would substantially reduce the probability of this type of failure.

It seems possible that with the new pitch axis gains and mechanization steps could be taken within the hardware to minimize the probability of such a failure occurring to a low enough level so that it may be neglected.

MH therefore proposes that in conjunction with the study of the new limit function for use with the new gains ti also studies to determine the practibility of lowering the probability of this error.

6.5 Effects of Gross Weights on Limit Load Factor

It is understood that some pad exists between the flight envelope limit load factor and the deformation limit of the aircraft, it is suggested that AVRO reduce this pad to a minimum.

Considering the wide gross weight range of the CF-105, it seems unlikely that one limit will protect at high gross weights and yet not prove a hinderance at the lower gross weights.

MH therefore wishes to propose for AVRO's consideration a relatively simple mechanization which has been used successfully previously to meet such a situation.

6.5 (cont.)

Use is suggested of a differential limit load factor which would be controlled by an aircraft system sensing gross wiehgt. The gross weight system would be redundent and failure of same would result in the lower of the two limits.

For example a dual microswitch with normally closed contacts wired in series would sense whether or not the belly tank is in place. Similar methods would sense other changes in gross weight commanding one limit or the other from the g limiter.

6.6 Possible Steps to Improve the Shaping of the N_z vs δ_s curves.

One of the reasons that it has been difficult to obtain a curve like figure 20 of section 5.3 is the high $\dot{\delta}_{e_{max}}$ relative to the amount of system dead time. Assuming for the moment that this could be reduced somewhat, lowering the break frequency on the high-passed servo position feedbacks may make it possible to approach the results of figure 20 section 5.3.

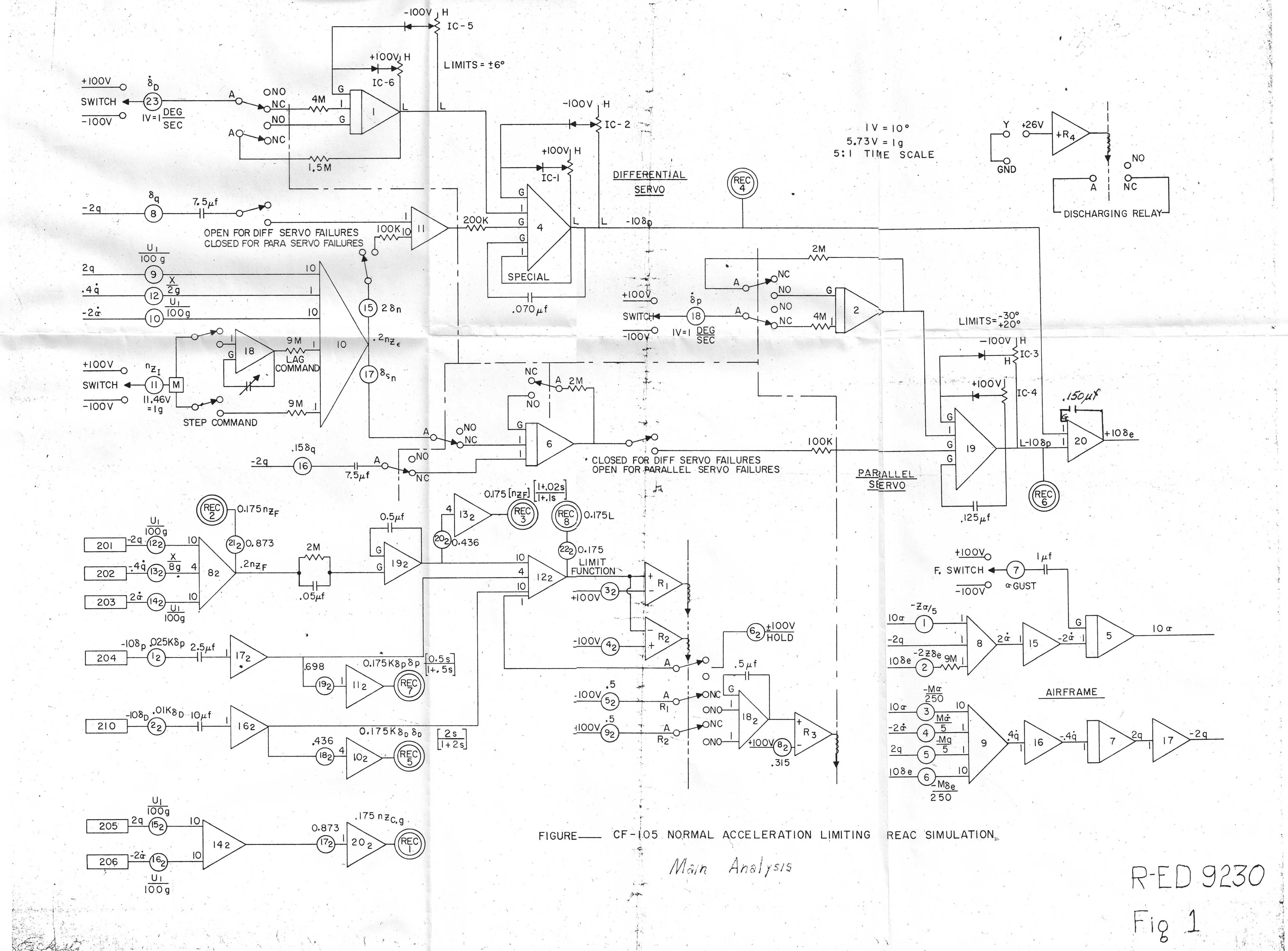

FIGURE—— CF-105 NORMAL ACCELERATION LIMITING REAC SIMULATION

Main Analysis

R-ED 9230

Fig 1

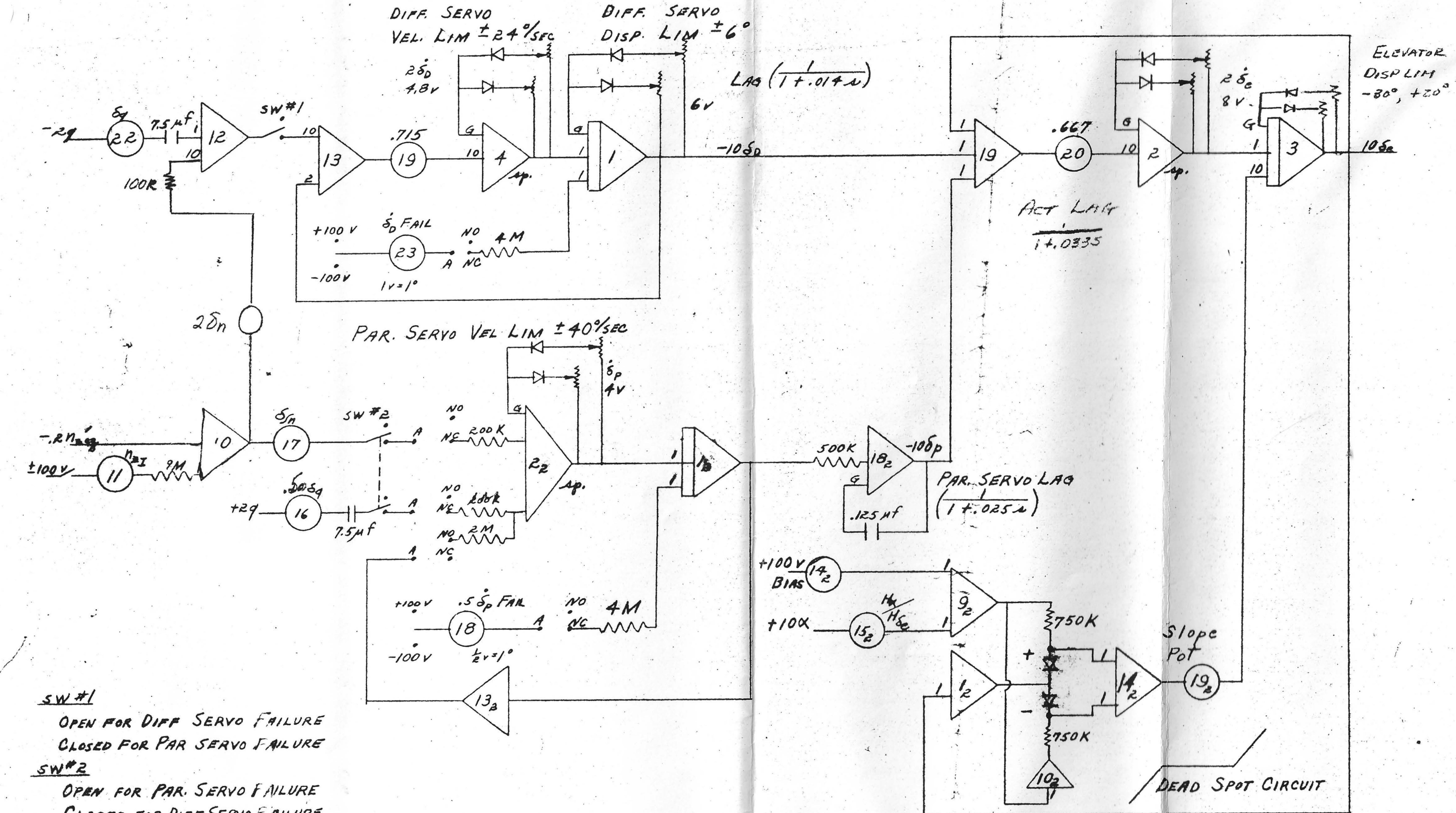

SW #1

OPEN FOR DIFF SERVO FAILURE

CLOSED FOR PAR SERVO FAILURE

SW #2

OPEN FOR PAR. SERVO FAILURE

CLOSED FOR DIFF. SERVO FAILURE

5.73ᵛ = 1 RAD = 1 g

1ᵛ = 10°

TIME SCALE 5:1

CF-105 G LIMITING REAC DIAGRAM

3rd Revision Sh 1

R-ED 9230

Fig 2

12/4/57

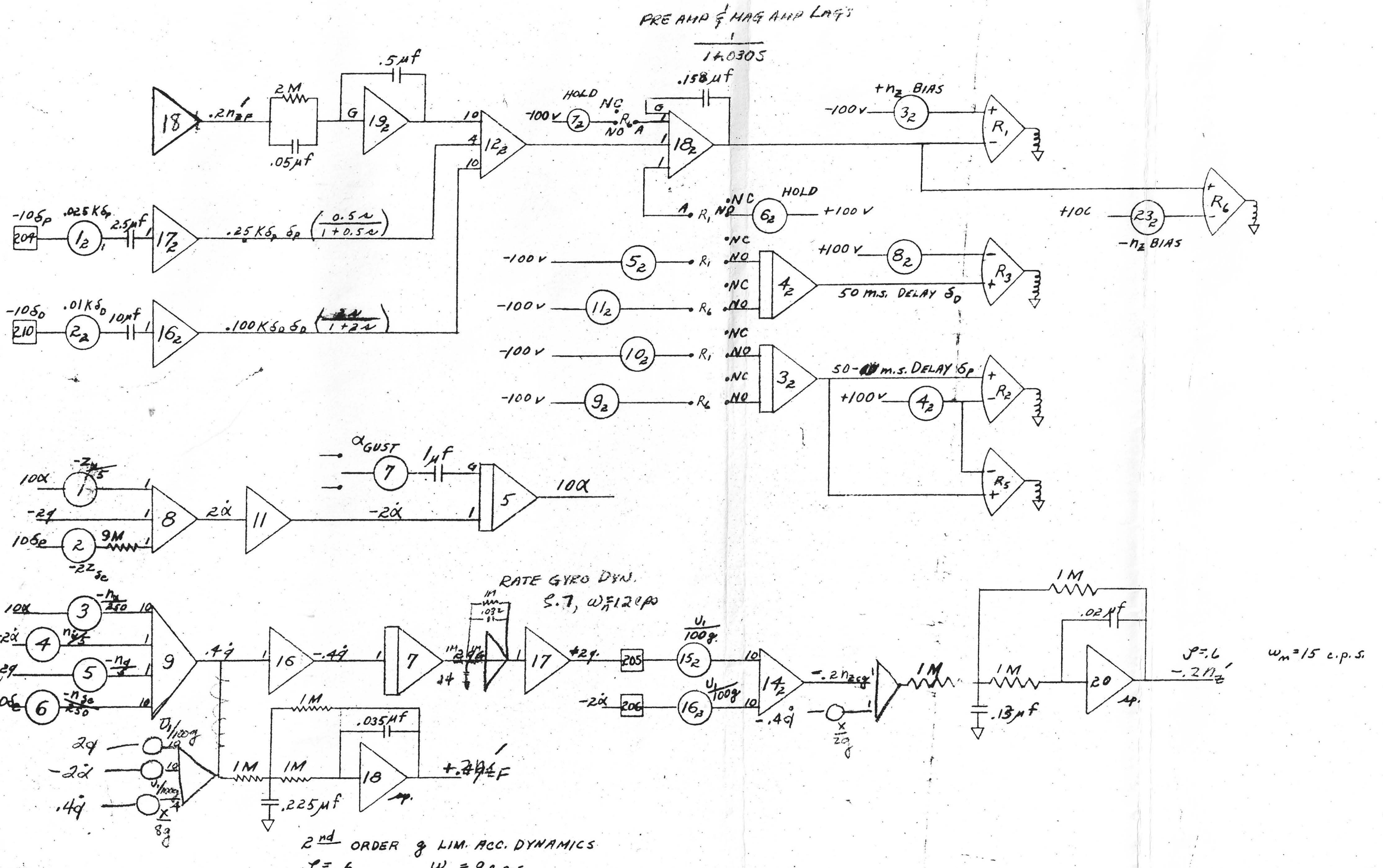

TIME SCALE 5:1

CF-105 G LIMITING REAC DIAGRAM
3rd Revision Sh 2

R-ED 9230
Fig 3
12/4/57

$$L = \left(\Delta n_{z_{c.g}} + \frac{162}{g}\dot{q}\right)\left[\frac{1+.02s}{1+.1s}\right] + 15.75\,\delta_P\left[\frac{.5s}{1+.5s}\right] + 12.5\,\delta_D\left[\frac{2s}{2s+1}\right]$$

CONDITION O-7

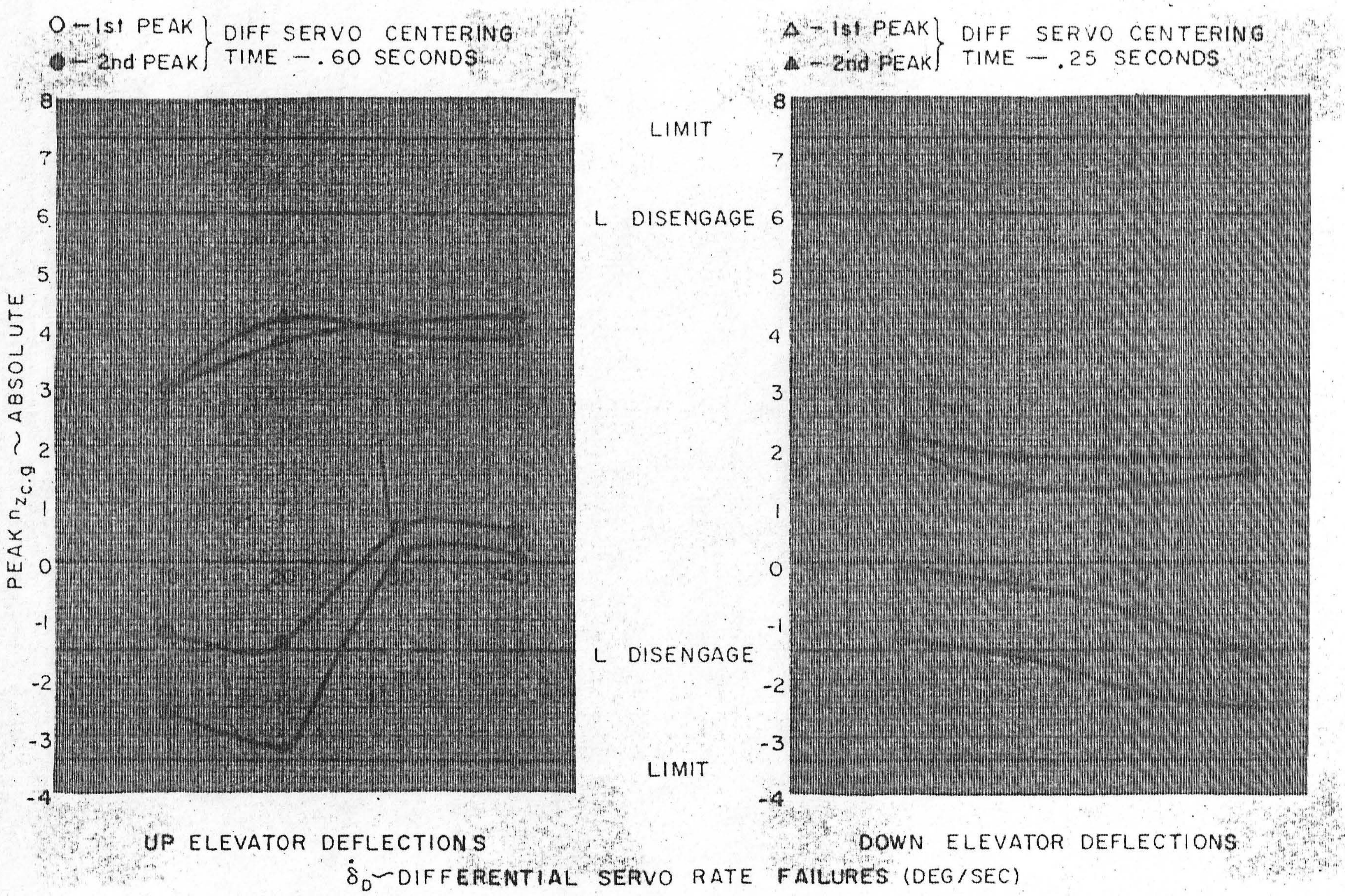

FIGURE 4 CF-105 NORMAL ACCELERATION LIMITING
PEAK NORMAL ACCELERATION VS DIFFERENTIAL SERVO RATE

RED 9230

$$L = \left(\Delta n_{z\,c.g} + \frac{162}{g}\dot{q}\right)\left[\frac{1+.02s}{1+.1s}\right] + 15.75\,\delta_p\left[\frac{.5s}{1+.5s}\right] + 12.5\,\dot{\delta}_D\left[\frac{2s}{2s+1}\right]$$

CONDITION 0-1.09

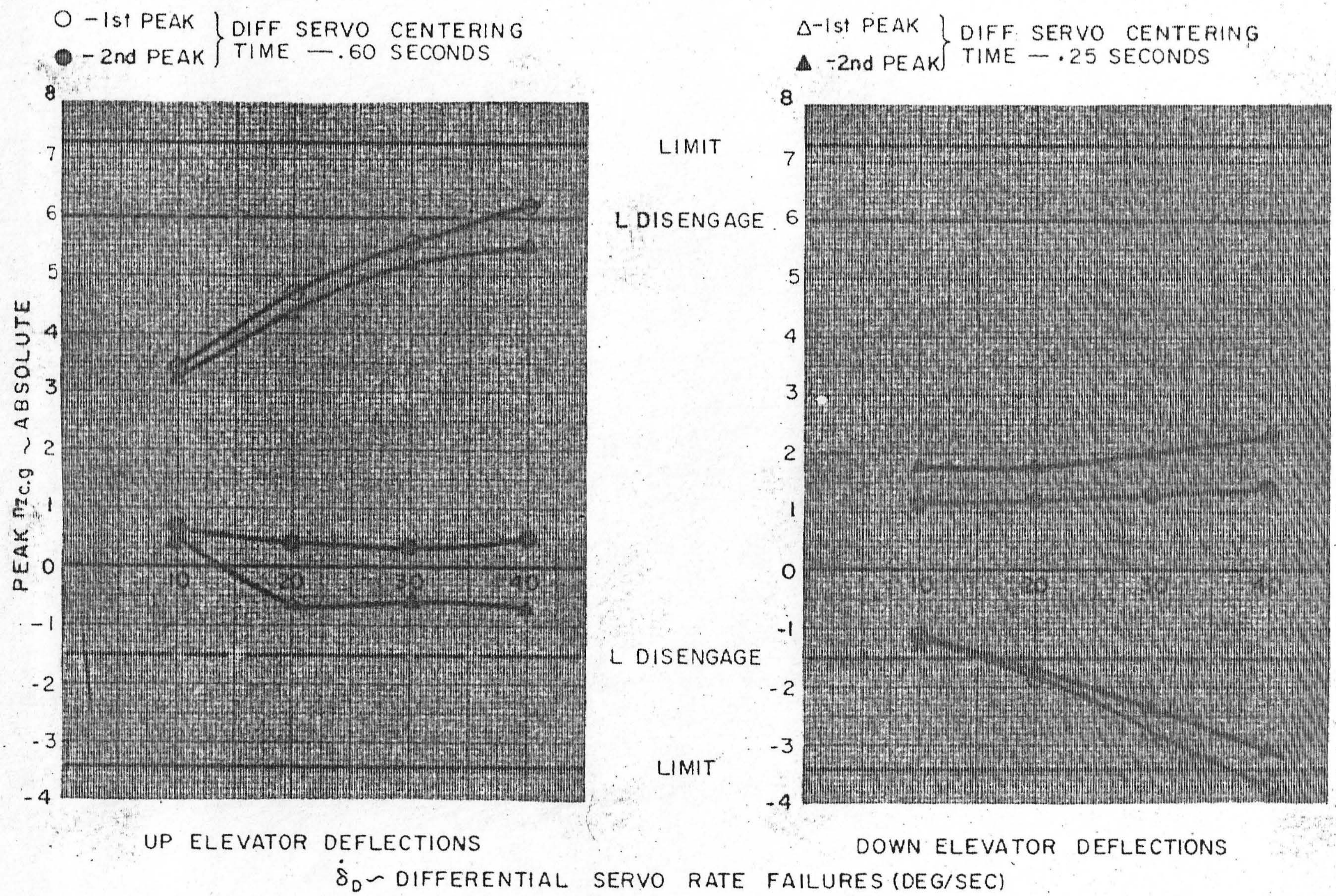

FIGURE 5 CF-105 NORMAL ACCELERATION LIMITING
PEAK NORMAL ACCELERATION VS. DIFFERENTIAL SERVO RATE

RED 9230

$$L = \left(\Delta n_{z\,c.g} + \frac{162}{g}\dot{q}\right)\left[\frac{1+.02s}{1+.1s}\right] + 15.75\,\delta_P\left[\frac{.5s}{1+.5s}\right] + 12.5\,\delta_D\left[\frac{2s}{2s+1}\right]$$

CONDITION 10-1.0

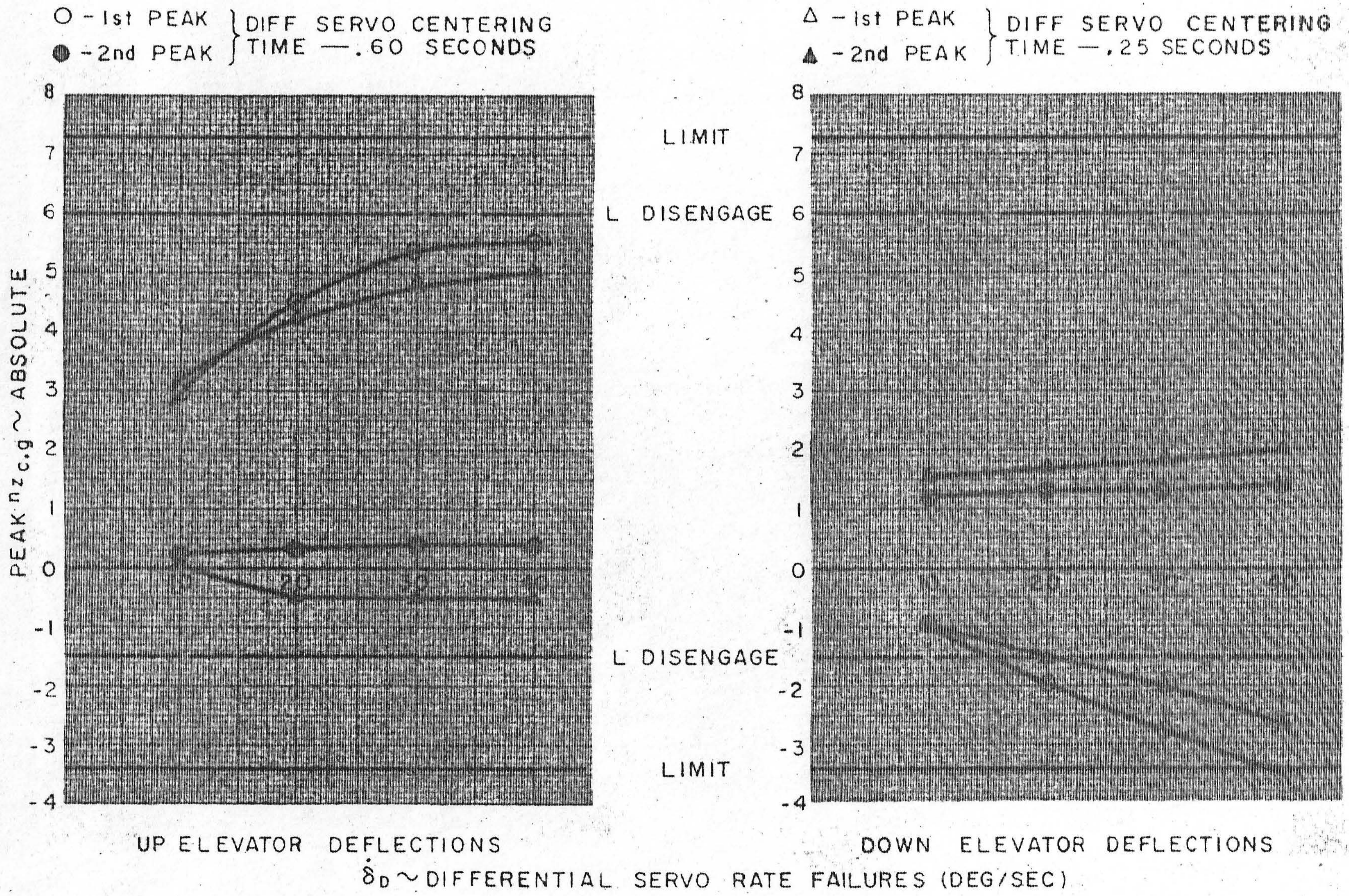

FIGURE 6 CF-105 NORMAL ACCELERATION LIMITING
PEAK NORMAL ACCELERATION VS. DIFFERENTIAL SERVO RATE

RED 9230

$$L = \left(\Delta n_{z_{c.g}} + \frac{162}{g} \dot{q} \right) \left[\frac{1 + .02s}{1 + .1s} \right] + 15.75\, \delta_p \left[\frac{.5s}{1 + .5s} \right] + 12.5\, \delta_D \left[\frac{2s}{2s + 1} \right]$$

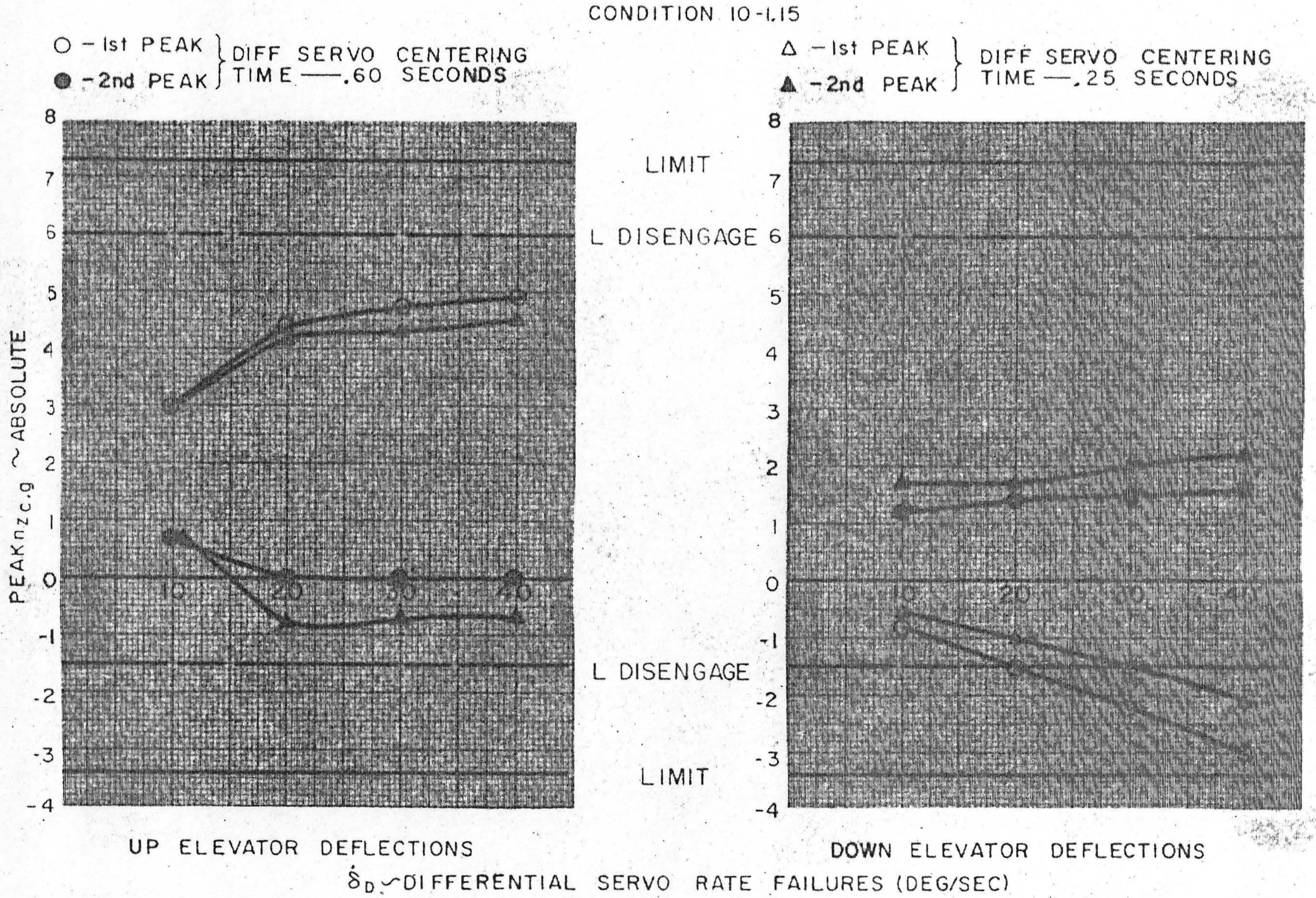

FIGURE 7 CF-105 NORMAL ACCELERATION LIMITING
PEAK NORMAL ACCELERATION VS. DIFFERENTIAL SERVO RATE

R-ED 9230

MH AERO REPORT 01196-02 TR4

$$L = \left(\Delta n_{z_{c.g}} + \frac{162}{g}\dot{q}\right)\left[\frac{1+.02s}{1+.1s}\right] - 15.75\,\delta_P\left[\frac{.5s}{1+.5s}\right] - 12.5\,\delta_D\left[\frac{2s}{2s+1}\right]$$

CONDITION 20-.9

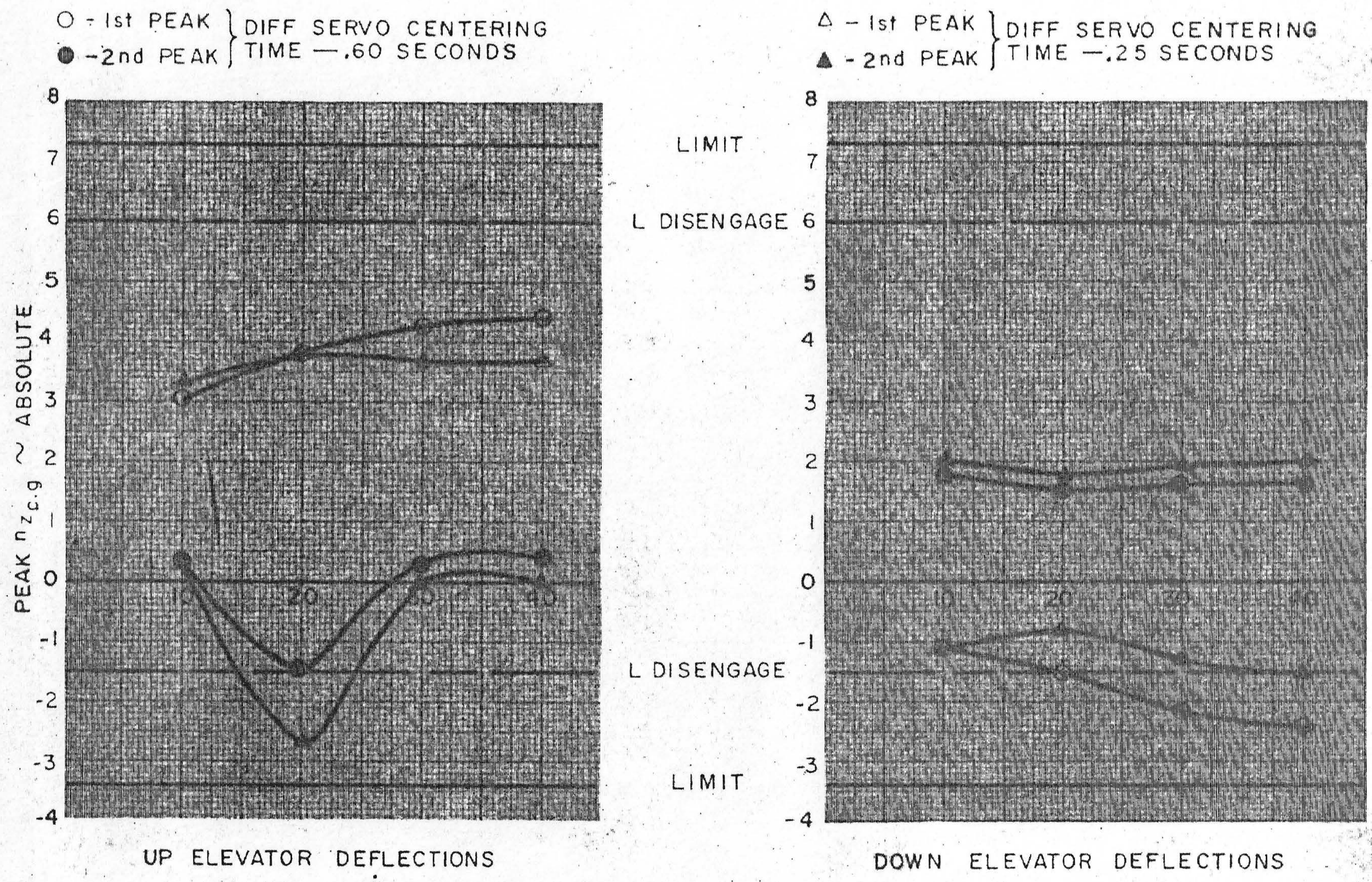

FIGURE 8 CF-105 NORMAL ACCELERATION LIMITING
PEAK NORMAL ACCELERATION VS. DIFFERENTIAL SERVO RATE

R-ED 9230

MH AERO REPORT C1196-02 TR4

$$L = \left(\Delta n_{z_{c.g}} + \frac{162}{g}\dot{q}\right)\left[\frac{1+.02s}{1+.1s}\right] + 15.75\,\delta_P\left[\frac{.5s}{1+.5s}\right] + 12.5\,\delta_D\left[\frac{2s}{2s+1}\right]$$

CONDITION 20-1.15

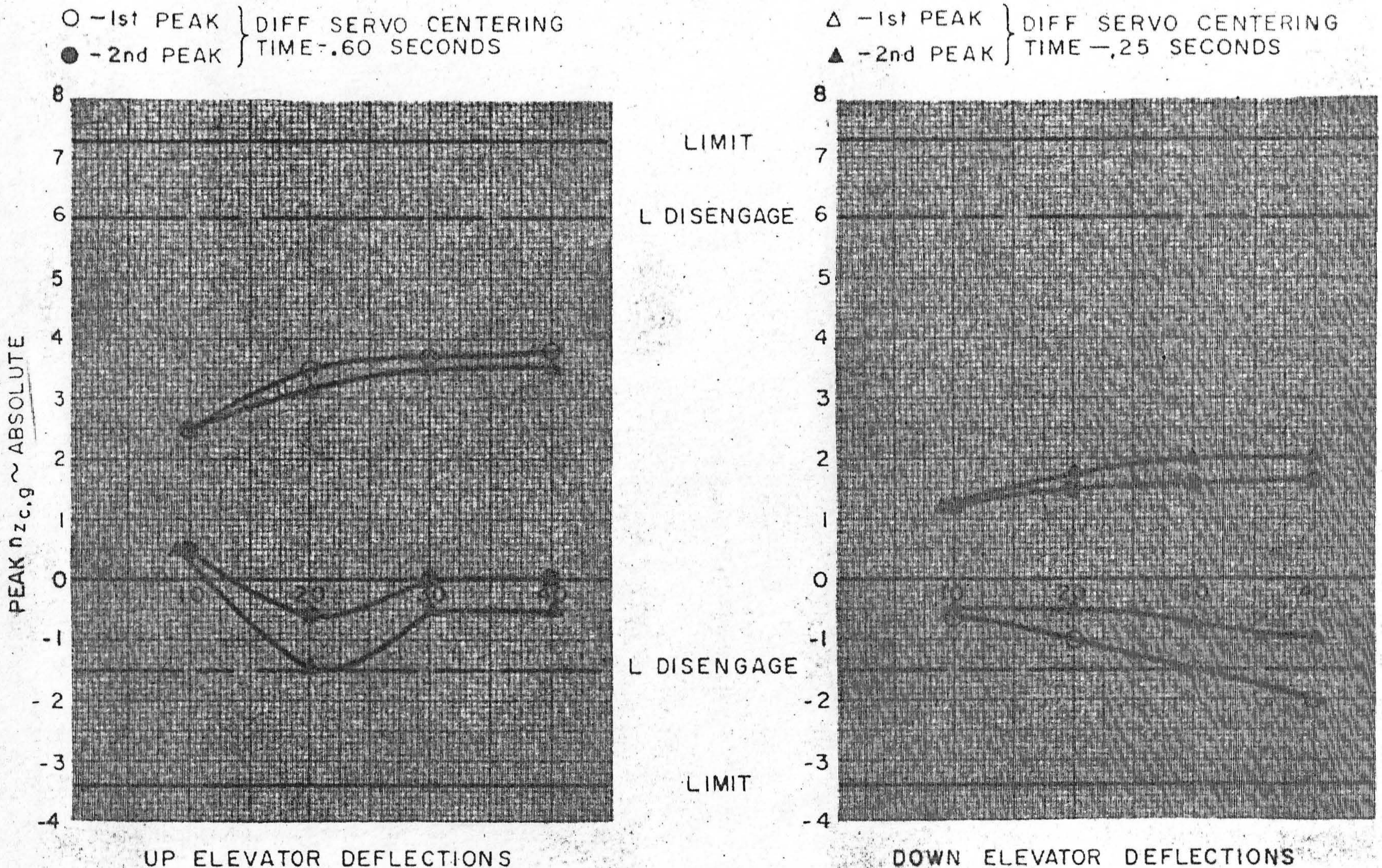

δ_D ~ DIFFERENTIAL SERVO RATE FAILURES (DEG/SEC)

FIGURE 9 CF-105 NORMAL ACCELERATION LIMITING
PEAK NORMAL ACCELERATION VS. DIFFERENTIAL SERVO RATE

R-ED 9230

MH AERO REPORT 01196-02 TR4

$$L = \left(\Delta n_{z_{c.g}} + \frac{162}{g}\dot{q}\right)\frac{1+.02s}{1+.1s} + 15.75\,\delta_p\,\frac{.5s}{1+.5s} + 12.5\,\delta_D\,\frac{2s}{2s+1}$$

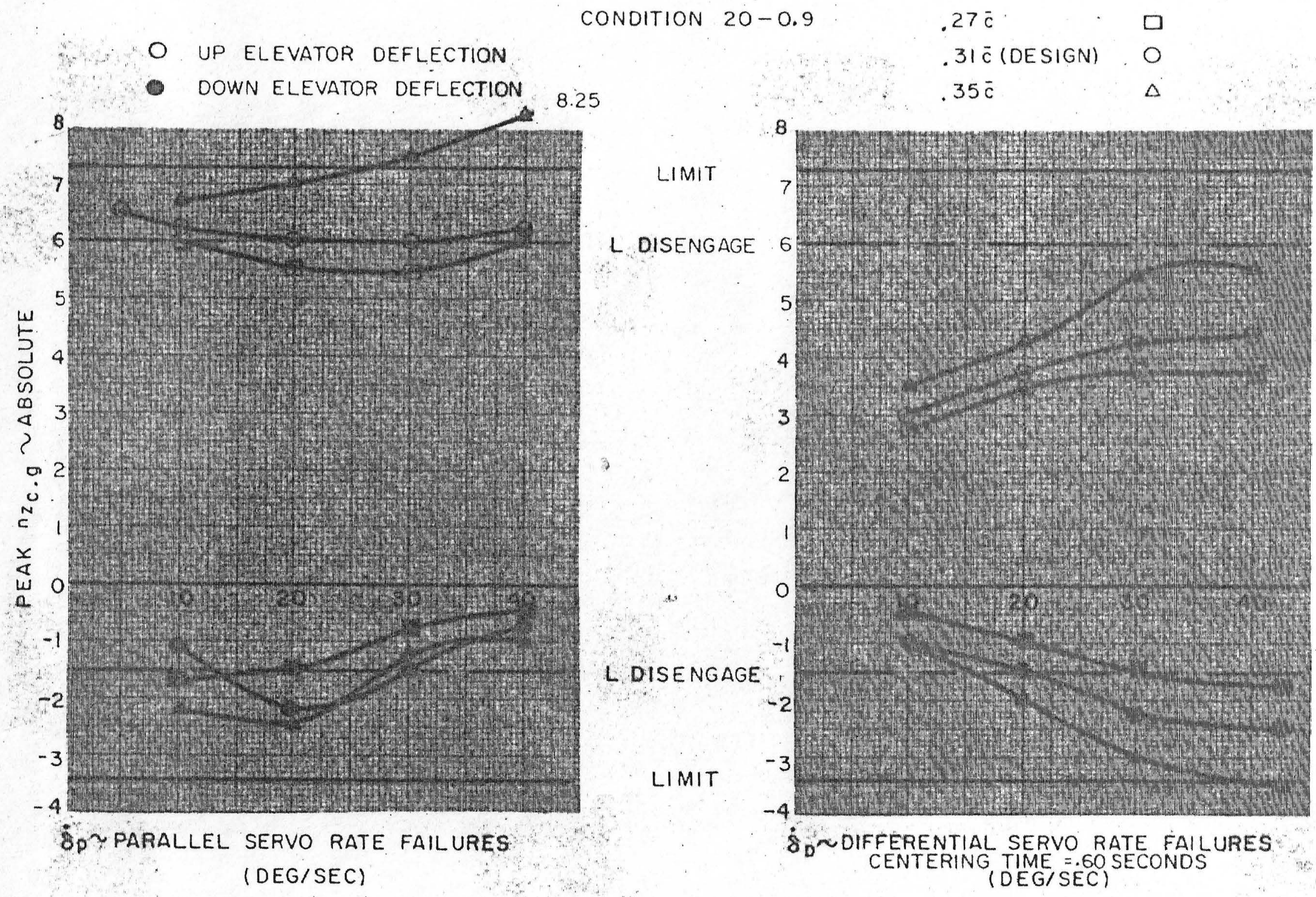

FIGURE 10 CF-105 NORMAL ACCELERATION LIMITING
PEAK NORMAL ACCELERATION VS. SERVO RATES

R-ED 9210

$$L = \left(\Delta n_{z_{c.g}} + \frac{162}{g}\dot{q}\right)\left[\frac{1+.02s}{1+.1s}\right] + 15.75\,\delta_p\left[\frac{.5s}{1+.5s}\right] + 12.5\,\delta_D\left[\frac{2s}{2s+1}\right]$$

CONDITION 10-1.3

○ UP ELEVATOR DEFLECTION

● DOWN ELEVATOR DEFLECTION

.27c̄ □

.31c̄ (DESIGN) ○

.35c̄ △

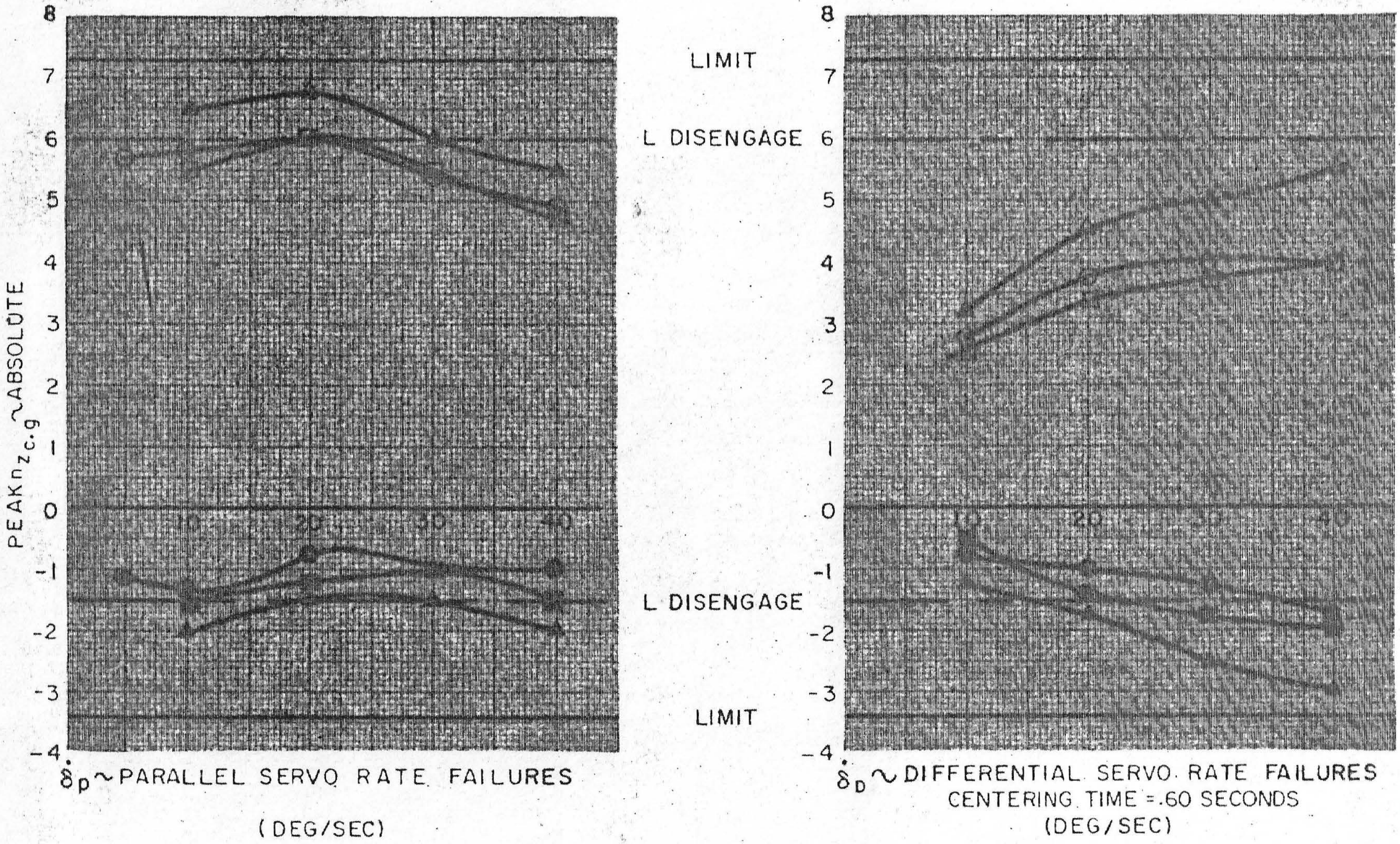

FIGURE 11 CF-105 NORMAL ACCELERATION LIMITING
PEAK NORMAL ACCELERATION VS. SERVO RATES

R-ED 9210

$$L = \left(\Delta n_{z_{c.g}} + \frac{162}{g}\dot{q}\right)\left[\frac{1+.02s}{1+.1s}\right] + 15.75\,\delta_p\left[\frac{.5s}{1+.5s}\right] + 12.5\,\delta_D\left[\frac{2s}{2s+1}\right]$$

CONDITION 0-1.09

○ UP ELEVATOR DEFLECTION

● DOWN ELEVATOR DEFLECTION

.27 $\bar{c}$ □

.31 $\bar{c}$ (DESIGN) ○

.35 $\bar{c}$ △

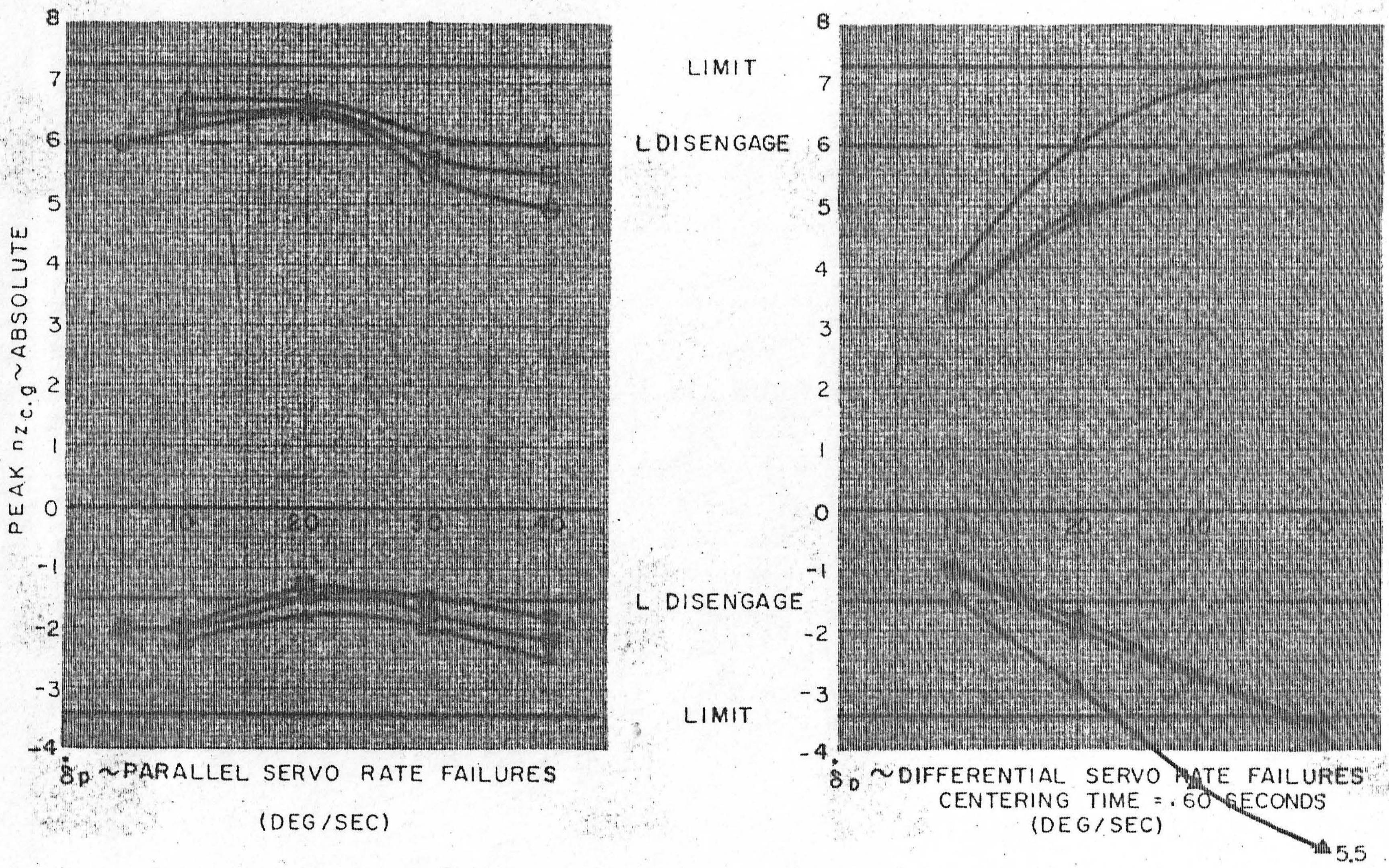

FIGURE 12 CF-105 NORMAL ACCELERATION LIMITING
PEAK NORMAL ACCELERATION VS. SERVO RATES

R-ED 9210

$$L = \left(\Delta n_{z_{c.g}} + \frac{162}{g}\dot{q}\right)\left[\frac{1+.02s}{1+.1s}\right] + 15.75\,\delta_P\left[\frac{.5s}{1+.5s}\right] + 12.5\,\delta_D\left[\frac{2s}{2s+1}\right]$$

CONDITION 0-1.09

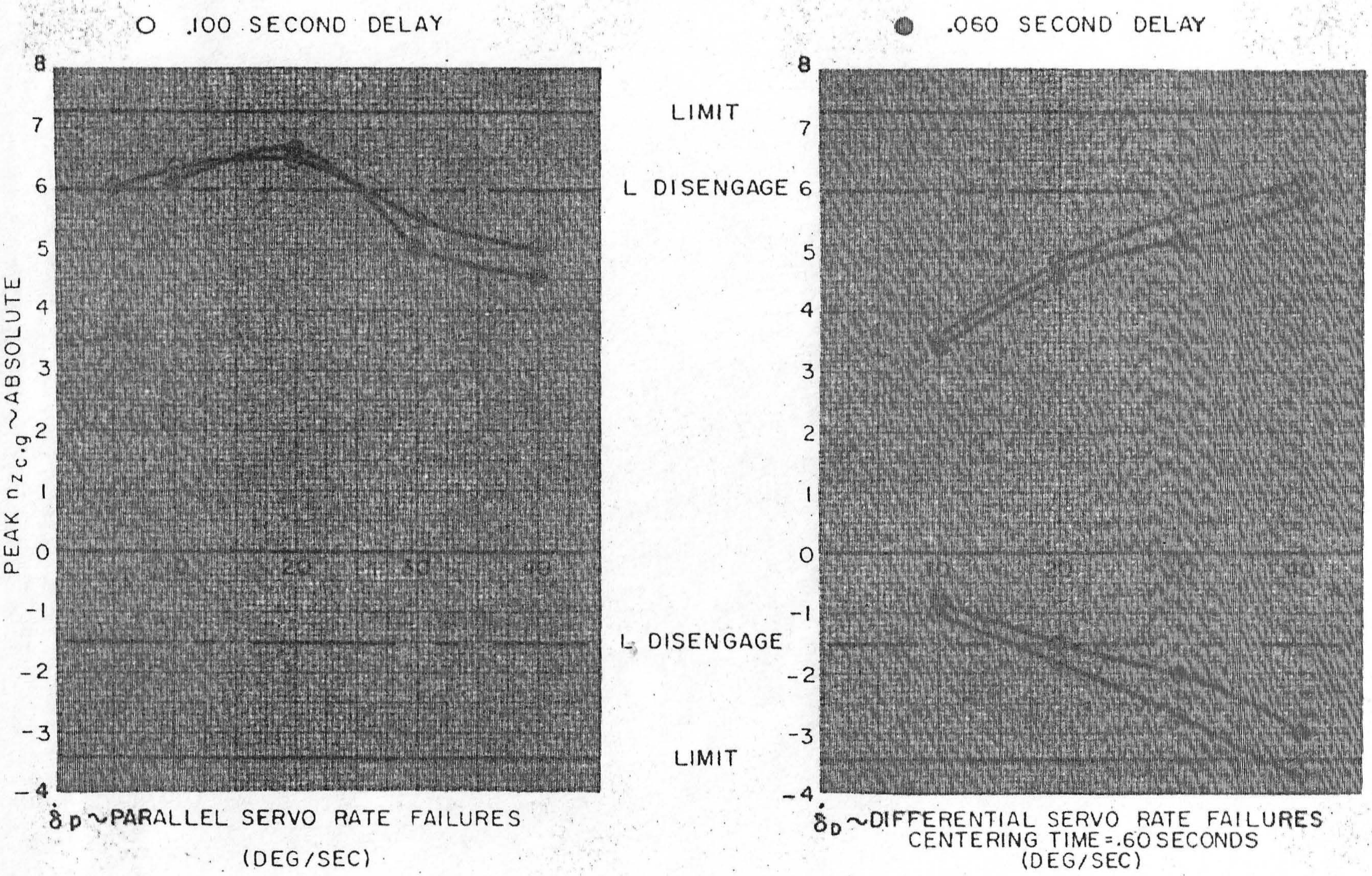

FIGURE 13 CF-105 NORMAL ACCELERATION LIMITING
PEAK NORMAL ACCELERATION VS. SERVO RATES

RED 9210

MH AERO REPORT 01196-02 TR4

$$L = \left(\Delta n_{z_{c.g}} + \frac{162}{g}\dot{q}\right)\left[\frac{1+.02s}{1+.1s}\right] + 15.75\,\delta_P\left[\frac{.5s}{1+.5s}\right] + 12.5\,\delta_D\left[\frac{2s}{2s+1}\right]$$

CONDITION 20-0.9

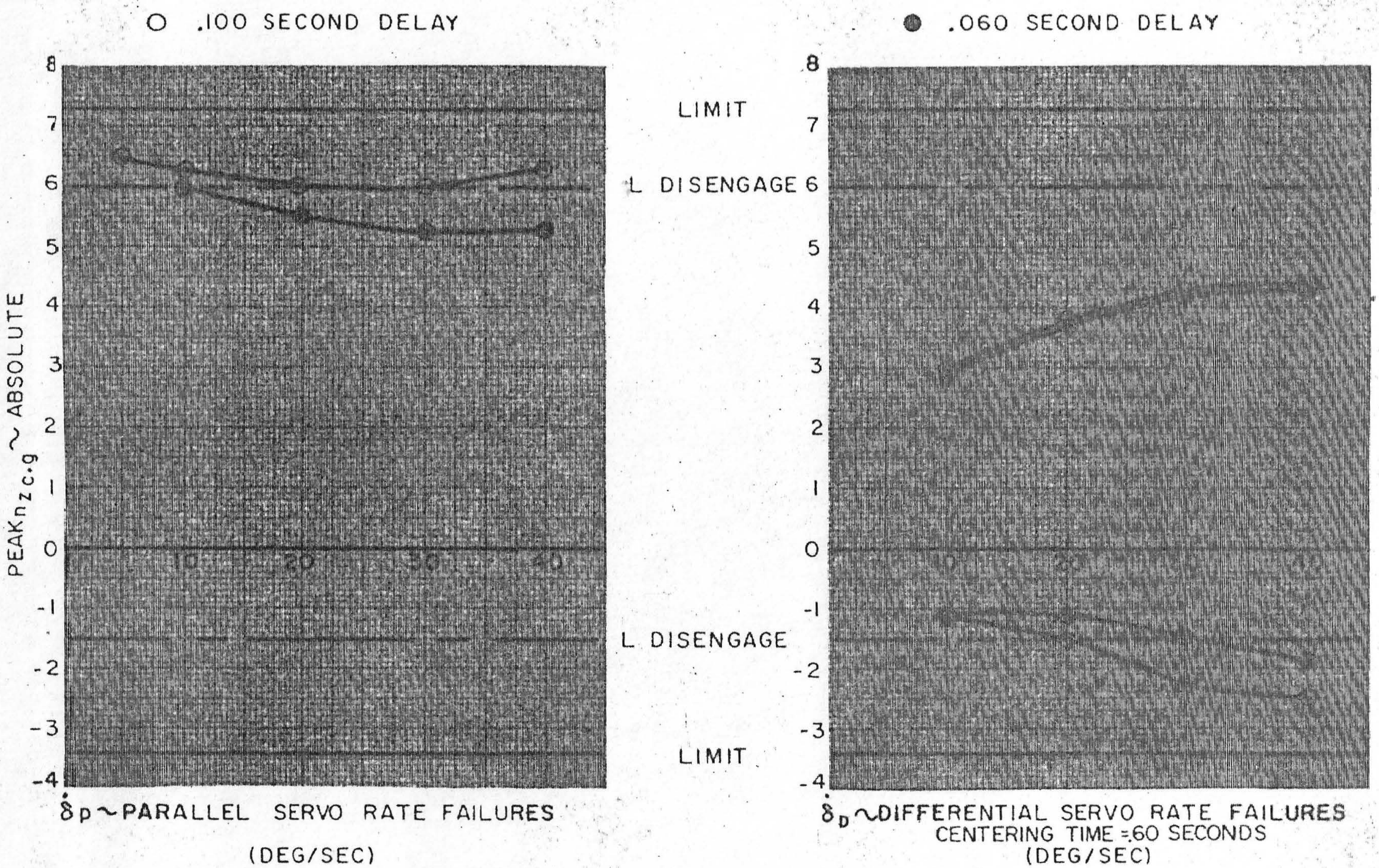

MH AERO REPORT 01196-02 TR4

FIGURE 14 CF-105 NORMAL ACCELERATION LIMITING
PEAK NORMAL ACCELERATION VS. SERVO RATES

R-ED 9210

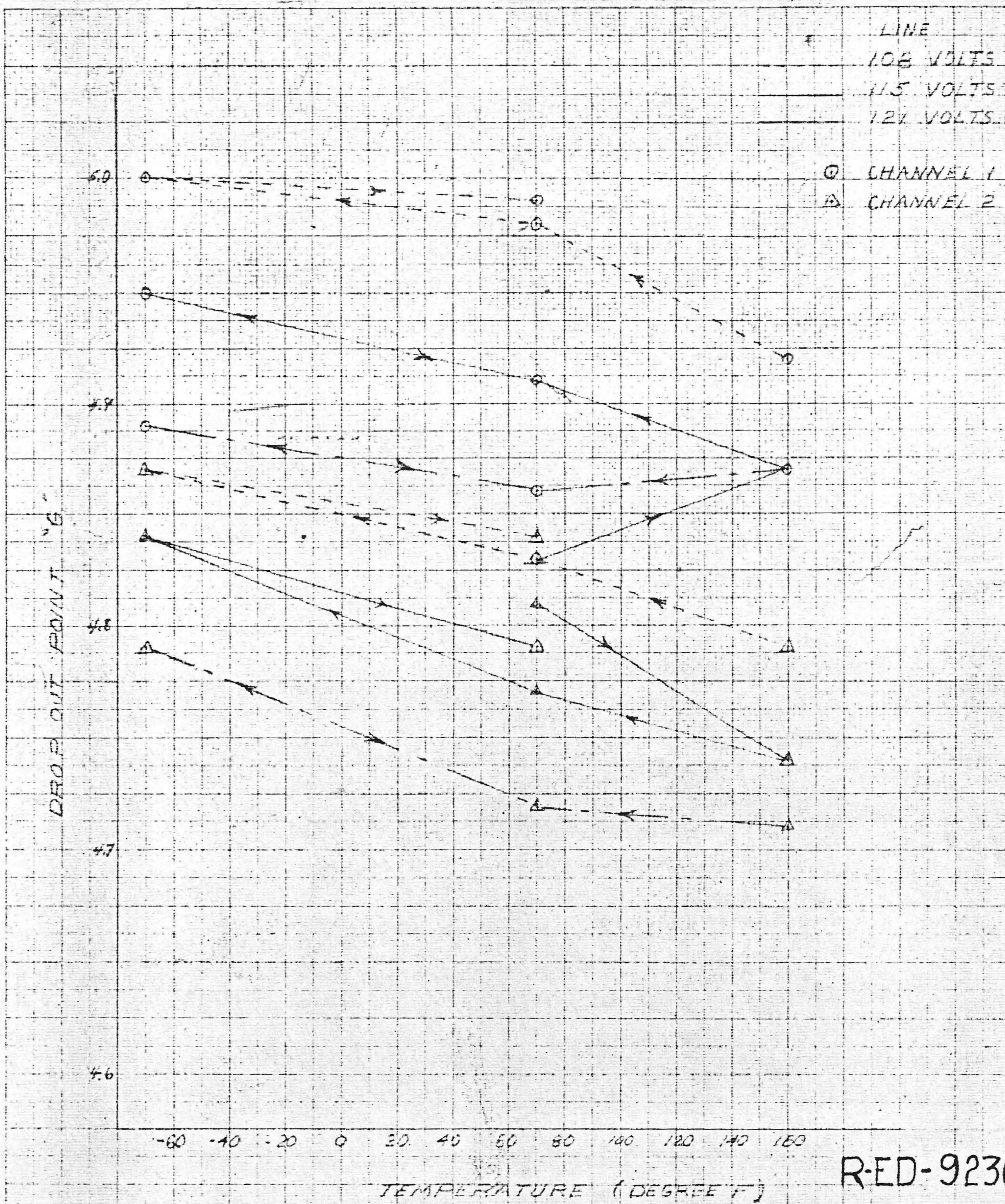

R-ED-9230

Fig. 15

AERONAUTICAL DIVISION MINNEAPOLIS-HONEYWELL REGULATOR COMPANY	TITLE: TEMPERATURE AND VOLTAGE CHARACTERISTICS OF XBG-67B-1 SERIES T1, S/N N-1	DATE: 1-12-56	GRAPH NO. 1
DEPARTMENT: TEST — CLASSIFICATION: U		DRAWN BY: EJW	DEV. NO. AD5251E
		TEST NO. AEX 21007	

98-2346

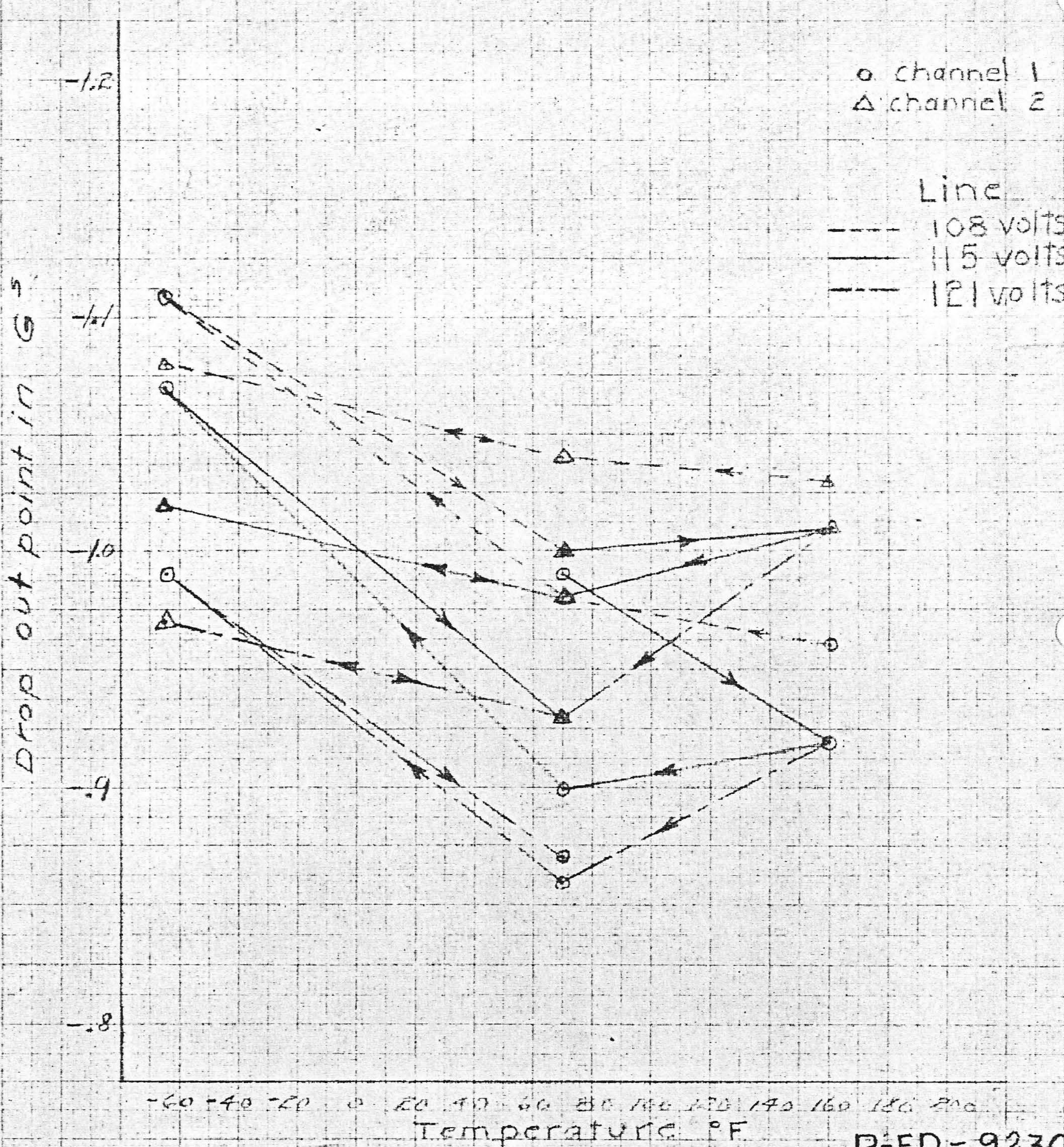

R-ED-9230
Fig 16

AERONAUTICAL DIVISION MINNEAPOLIS-HONEYWELL REGULATOR COMPANY	TITLE: Temperature & voltage characteristic of XBG 67B-1 SERIES T 1, S/N N-1	DATE: 1-12-56	GRAPH NO. 2
		DRAWN BY: LMF	DEV. NO AD5251E
DEPARTMENT: Test	CLASSIFICATION: U	TEST NO. AEX 21087	

46-2346

Pre-Amplifier Errors

EG 155A

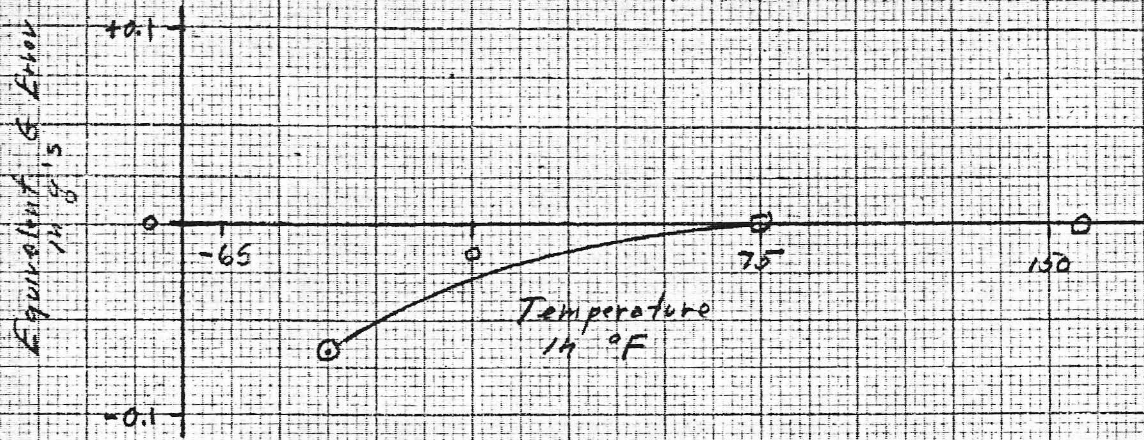

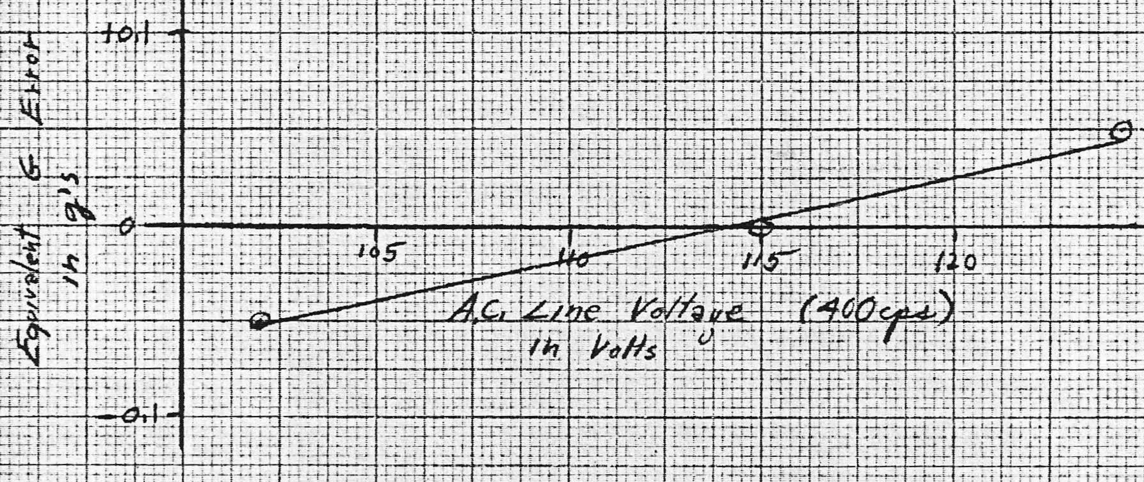

R-ED 9230

Fig 17

Cond 20.9

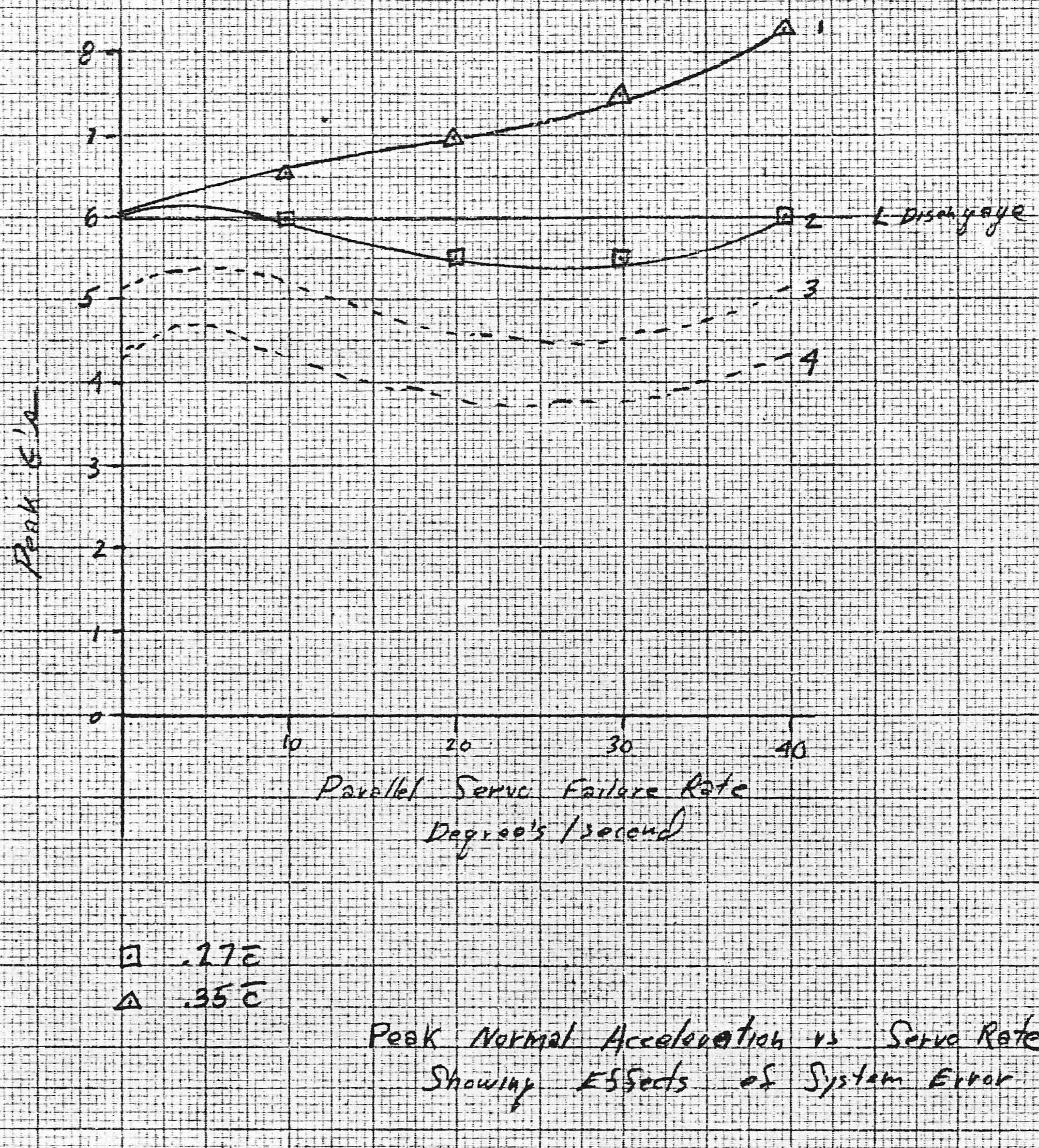

Peak Normal Acceleration vs Servo Rate
Showing Effects of System Error

R-FD 9230

Fig 18